LIMNOLOGY and OCEANOGRAPHY

ASLO

Limnol. Oceanogr. 68, 2023, S87–S100

doi: 10.1002/lno.12261

A positive temperature-dependent effect of elevated CO_2 on growth and lipid accumulation in the planktonic copepod, *Calanus finmarchicus*

David M. Fields [1*] Jeffrey A. Runge [2] Cameron R. S. Thompson [2,3] Caroline M. F. Durif [3] Steven D. Shema [3] Reidun M. Bjelland [3] Maura Niemisto [1] Michael T. Arts [4] Anne Berit Skiftesvik [3] Howard I. Browman [3]

[1]Bigelow Laboratory for Ocean Sciences, East Boothbay, Maine
[2]Darling Marine Center, School of Marine Sciences, University of Maine, Walpole, Maine
[3]Ecosystem Acoustics Group, Institute of Marine Research, Austevoll Research Station, Storebø, Norway
[4]Department of Chemistry and Biology, Toronto Metropolitan University, Toronto, Ontario, Canada

Abstract

Calanus finmarchicus were reared from eggs to adults at 12°C and 16°C with non-limiting food in combination with ambient (600 μatm) and high (1100 μatm) pCO_2. These conditions are likely to be encountered by the species at the southern margins of its biogeographical range by the end of the century. Dry weight (DW), carbon (C) and nitrogen (N) mass, oil-sac volume (OSV), fatty acid composition (FA), and oxygen consumption rates (OCR) were measured on newly molted stage CV copepodites and recently molted adult females. By focusing our measurements on these precise events in the life cycle, we were able to obtain a more accurate comparison of growth and respiration across treatments. Copepods raised at 12°C had a significantly greater DW, OSV, and C and N mass than those raised at 16°C High pCO_2, independent of temperature, was associated with a further increase in the DW and C content of the copepods. Interactive effects of temperature and pCO_2 resulted in a larger OSV at low temperature and high pCO_2. Mass-specific respiration rates were significantly lower at lower temperatures and elevated pCO_2 suggesting that the increase in mass (DW, C, and OSV) resulted from reduced metabolic cost. The composition of fatty acids in the copepods varied mainly with temperature. Two fatty acids varied with pCO_2: 16:0 tended to decrease with higher pCO_2 and 18:3n−3 tended to increase with higher pCO_2. These observations suggest that elevated pCO_2/lower pH in future oceans may have a beneficial effect on *C. finmarchicus*.

The addition of anthropogenic carbon into the atmosphere has caused the oceans to warm and acidify, but the joint effects of these changes remain unclear for the majority of marine species (Caldeira and Wickett 2003; Browman 2017). Changes in pH and temperature are not uniform across the marine environment. Higher latitudes are experiencing both sharper decreases in pH and more rapid increases in temperature than lower latitudes (Fabry et al. 2008). Over the past several decades, the North Atlantic has warmed more rapidly than the global average, including notable heat waves in 2012 and 2018 (Pershing and Stamieszkin 2020). Although temperature is a well-studied determinant of growth, development, and survival in crustaceans (Ross and Quetin 1988; Anger 2001; Quinn 2017), studies of responses to an elevated partial pressure of carbon dioxide (pCO_2) are fewer and more recent. It has become clear that responses to these two environmental drivers are species and life-stage specific, and that their effects can be interactive (reviewed by Whiteley 2011; Gledhill et al. 2015; Wang et al. 2018).

The planktonic copepod *Calanus finmarchicus* is a dominant contributor to mesozooplankton biomass in the North Atlantic Ocean and is a foundational species in the subarctic North Atlantic ecosystem (Melle et al. 2014; Pershing and Stamieszkin 2020). Early life stages of *C. finmarchicus* serve as food for fish larvae and older, lipid-rich, stages nourish

*Correspondence: dfields@bigelow.org

Additional Supporting Information may be found in the online version of this article.

Author Contribution Statement: D.M.F., J.A.R., M.T.A., A.B.S., and H.I.B. conceived and designed the experiments and provided funding for the project. All authors performed the experiments, analyzed the data, prepared, figures and/or tables, authored or reviewed drafts of the paper, and approved the final draft.

Special Issue: Cascading, Interactive, and Indirect Effects of Climate Change on Aquatic Communities, Habitats, and Ecosystems. *Edited by: Susanne Menden-Deuer, Maarten Boersma, Hans-Peter Grossart, Ryan Sponseller, Sarah A. Woodin and Deputy Editors Julia C. Mullarney, Steeve Comeau, and Elisa Schaum.*

planktivorous forage fish (Heath and Lough 2007; Buren et al. 2014; Lindegren et al. 2018; Staudinger et al. 2020), and the endangered North Atlantic right whale (Record et al. 2019). The species' success lies, in part, in its ability to overwinter from late summer to mid-winter in order to survive this period of high predation and low food availability. To survive without food *C. finmarchicus* accumulates a large reserve of lipids during the spring–summer (Sargent and Henderson 1986; Hirche 1996; Jónasdóttir 1999) and transitions to a semi-dormant state with reduced metabolic activity at depth over winter. Its ability to accumulate lipids is key to winter survival and preparation for egg production the following spring. The lipid content of *C. finmarchicus* can reach up to 73% of their total dry weight; thus, it is a key food source for higher trophic levels in late spring through fall (Heath and Jónasdóttir 1999).

Although *C. finmarchicus* is sensitive to temperature increases, experiments conducted on copepods under predicted end-of-century pCO_2 concentrations have not generally produced adverse effects on physiological processes controlling birth and individual growth rates (Bailey et al. 2016, 2017; Runge et al. 2016 and references cited therein). Results of experiments in which *C. finmarchicus* was reared from egg to adult at 12°C suggested that increased pCO_2 enhances growth rate. Specifically, prosome length and body mass, in terms of carbon, nitrogen and dry weight, was marginally higher at 1200 μatm CO_2, although imprecision in the measurement of copepod body size at precisely the same age-within-stage across treatments precluded a definitive conclusion about a possible positive effect (Runge et al. 2016). The experimental approach used in the work reported here was designed to isolate a single developmental stage (CV) and assess the impact of temperature and pCO_2 on the growth, vital rates, and C, N, and lipid deposition during that stage. This novel method minimizes a source of variability that arises from sampling rapidly growing individuals of varying and unknown age within a single developmental stage. This source of error is particularly acute for *C. finmarchicus* during stage CV because the mass of an individual nearly doubles between the start and end of this stage. To address this, we measured biological endpoints on newly molted stage CVs (within 12 h) and again once the copepod molted to stage CVI (within 12 h). Comparing biological endpoints from animals within narrow age limits makes it possible to identify small differences between treatments.

The possibility that higher temperature and elevated pCO_2, have direct and interactive effects on the vital rates is understudied (Breitburg et al. 2015; Wang et al. 2018). Here, we present the results of an experiment designed to test whether moderately elevated pCO_2 levels and temperature affect the size, lipid accumulation, and respiration rates of *C. finmarchicus*.

Methods

The experiment was conducted at the Austevoll Research Station, Institute of Marine Research, Norway (60.086°N, 5.262°E). The experimental design was full-factorial, consisting of two nominal temperatures (12°C and 16°C) and three replicate tanks at each of two pCO_2 treatments: ambient (at seawater source) and high (nominally 1100 μatm) at each temperature. The source of seawater was the station's flowing seawater system, which draws water from the adjacent Bjørnafjord at a depth of 160 m. The ambient pH ($_{NBS}$) of seawater at the intake depth is ~7.95, corresponding to a pCO_2 of ~590 μatm. In the laboratory's preparation room, a high pCO_2 stock seawater solution was maintained at a pH of ~5.8. This stock solution was mixed into holding tanks (100 L) to create seawater targeting the nominal treatment pCO_2 level. The pH levels in the treatment tanks were maintained at preset pH levels by adding stock solution to the tank using dosage pumps controlled by feedback from pH electrodes/controllers. The ambient control and pCO_2 treatment water in the holding tanks were then pumped to three header tanks for distribution to the ambient pCO_2 and treatment pCO_2 tanks in each of two temperature-controlled laboratories set at 12°C and 16°C, respectively. The 40-L experimental tanks, identical for all replicates, were 44 cm in diameter and made of high-density polyethylene. The inlet tube into each experimental tank was fitted with a 60-mm mesh nitex screen, cleaned periodically to prevent contamination. The flow rate of water into the experimental tanks varied between 5 and 12 L h^{-1} giving a retention time of 3.3–8 h for the water in the tank. The water in the experimental tanks drained through a screen (70 μm) placed over a perforated 35-mm diameter plastic standpipe running the height of the tank. This setup ensured very low exit flow rates at any point along the tube. The size of the exit screen was increased to 150 mm during the experiment because the copepods increased in size and would not be washed out with a larger mesh size. Early life stage copepods in close vicinity of the exit pipe could easily swim away and were not sucked into the drain pipe. This system provided a sufficiently gentle environment for rearing copepod life stages while maintaining high water replacement within the tanks and stable pCO2 treatment levels. Details of the system are provided in Runge et al. (2016). The realized experimental conditions are provided in Table 1.

Procedures for initiation of the experiment followed the method described in Runge et al. (2016). Briefly, copepods were collected using light traps (500 μm mesh) deployed at 15–20 m overnight off the dock of the Austevoll Research Station in late April 2015. Approximately 1000 female *C. finmarchicus* were sorted under a binocular microscope and distributed among several 10-L egg separation chambers. Examination of the interior margin of the P5 basipod (Frost 1974) in a subsample of the females indicated that < 5% of the females were the sibling species, *Calanus helgolandicus*. The females were fed a stock algal culture consisting of 60% *Rhodomonas baltica*, 25% *Skeletonema costatum*, and 15% *Chaetoceros mulleri* (by carbon content) at a concentration

Table 1. Mean carbonate chemistry during the 6-week incubation. Total alkalinity (A_T) and total inorganic carbon (C_T) were measured every 3–4 d in each replicate tank. Nutrient data from Runge et al. (2016) ambient control. Inorganic carbon, pCO_2, and $pH_{(Tot)}$ were calculated using CO2sys V2.1. $N = 108$ and 83 for cold and warm controls and treatments, respectively; numbers in parentheses represent mean standard error. Temperature (mean ± SD; $n = 43$), salinity (mean ± SD; $n = 43$) were measured daily and spec-pH (mean ± SD; $n = 10$) was measured twice a week.

Treatment (pCO_2)	Temp (°C)	A_T (μMol kg^{-1})	N (μMol kg^{-1})	P (μMol kg^{-1})	Si (μMol kg^{-1})	C_T (μMol kg^{-1})	HCO_3^- (μMol kg^{-1})	CO_3^{2-} (μMol kg^{-1})	CO_2 (μMol kg-^{1})	pCO_2 calculated (μatm)	$pH_{(Tot)}$ calculated
Control	12.3 (0.05)	2341 (2.0)	11.2	2.3	7.0	2192 (1.4)	2056 (2.0)	113.4 (0.8)	23.2 (0.2)	566 (5.5)	7.91 (0.004)
"Ambient cold"											
Treatment	12.0 (0.05)	2337 (2.4)	11.2	2.3	7.0	2272 (5.0)	2044 (8.4)	118.5 (3.4)	24.2 (1.4)	669 (37.2)	7.86 (0.02)
"High cold"											
Control	16.3 (0.08)	2340 (1.9)	11.2	2.3	7.0	2187 (6.3)	2159 (6.5)	71.7 (2.6)	41.7 (1.2)	1019 (29.4)	7.68 (0.01)
"Ambient warm"											
Treatment	16.3 (0.03)	2339 (1.5)	11.2	2.3	7.0	2276 (1.3)	2162 (1.4)	71.1 (0.6)	43.5 (0.5)	1200 (12.5)	7.62 (0.01)
"High warm"											

sufficient to support maximum feeding rates (>600 μg C L^{-1}). Egg laying rates after several days were ~40 eggs female^{-1} d^{-1}.

The experiment was designed as a three-way full factorial ANOVA with copepod stage (new CV, representing the cumulative effects up to stage CV, and new CVI, representing effects during stage CV), temperature (12°C and 16°C) and pCO_2 (600 and 1100 μatm) as independent variables. Each treatment had three replicate tanks (total—12 tanks). Beginning on 30 April, 2015, one replicate of the 600 pCO_2 treatment and one replicate of the 1100 pCO_2 treatment within the 12°C treatment was inoculated with *C. finmarchicus* eggs. Over the next 2 days, the second and third replicate tanks were inoculated. This was repeated for the 16°C tanks. The 12°C tanks were inoculated first to account for the longer development times at the lower temperature. This inoculation procedure ensured that all of the tanks received eggs from the same population of females and the staggered start dates gave the research team of four to six people sufficient time to sample and analyze each tank over the 45-d experiment. The inoculation procedure involved immersion (except for a lip above the surface to prevent escape of females) of several 0.75–l egg separation chambers into a tank over a 24-h period, allowing females to produce eggs, which entered the tank through the Nitex-screened floor of the chamber. Each tank was provided with ~10,000–15,000 eggs to provide enough adults for analysis assuming a 60% hatching success at these temperatures and pH (Preziosi et al. 2017), natural mortality, and removal of animals for sampling. The egg separation chambers, and each tank throughout the course of the experiment, were supplied with food ad libitum composed of the algal mixture described. The algal mixture used to feed the copepods was the same for all experimental tanks. The algae was introduced into the 40-L rearing tanks using a peristaltic pump system as described in Runge et al. (2016).

Measurement of tank conditions and analysis of carbonate chemistry closely followed protocols established in experiments conducted in the previous year, reported in Runge et al. (2016). Temperature and salinity in the tanks were measured daily with a handheld multimeter (Cond 340i conductivity meter: WTW). The pH level in each exposure tank was measured daily in a 100 mL sample using a Mettler Toledo pH meter equipped with a Mettler Toledo InLab ExpertPro pH-probe, calibrated with 4.00, 7.00, and 9.00 buffers (Certipur buffer solutions, Merck KGaA), traceable to standard reference material from NIST (NBS) (Andersen et al. 2013). The daily electrode pH (mV) was corrected to the spectrophotometrically determined pH (pHtot; see below) by plotting the mV from the pH electrode as a function of the (pHspec). The $pH_{(Tot)}$ was measured spectrophotometrically twice per week (Hitachi U-2900 dual-beam) using the pH-sensitive indicator dye m-cresol purple (Sigma-Aldrich) following SOP (standard operating procedure 6b: Dickson 2007). Carbonate chemistry was determined from total dissolved inorganic carbon (CT), total alkalinity (AT), temperature, salinity, and nutrients

(Runge et al. 2016). The nutrient samples for this experiment were lost, so we used nutrient data from the previous experiment (Runge et al. 2016) conducted under similar conditions. Carbonate chemistry parameters including pH(T) calculated using CO2SYS2.1 (Lewis et al. 1998) with the standard set of carbonate system equations and constants of Mehrbach et al. (1973) after applying the refit of Dickson and Millero (1987).

The copepods were fed the stock algal mixture, which was cultured in large-volume plastic bags (Bacaplast) at 22°C in the phytoplankton culture facility at the Austevoll Research Station. Daily subsamples from the batch cultures were counted and sized using a Z2 Beckman Coulter Counter. The food mixture was distributed from a 5-L reservoir to each tank using a peristaltic pump to maintain a nominal concentration of 600 μg C L^{-1}; taking into account the average water exchange rate of 10 L h^{-1}. Phytoplankton cell concentrations in each tank were monitored daily using a Moxi-Orflo cell counter with s-cartridges (Moxi-Orflo). Additional procedural details are provided in Runge et al. (2016).

The stage composition of *C. finmarchicus* in each tank was tracked daily by removing a subsample of animals and identifying them to stage. When the population in a tank started to reach the target stage CV, ~100 CIV individuals were sorted and isolated in a separate chamber within the tank. At the end of a 12-h incubation period, newly molted CV animals from this batch were either photographed and processed for further biometric measures or transferred to chambers for respiration rate measurements. Methods for photographic assessment of prosome length (PL) and oil sac volume (OSV), determination of dry weight (DW), and measurement of carbon and nitrogen mass are described in detail in Runge et al. (2016). In this study, the animals that were photographed were the same animals on which the other measurements were made. While PL and OSV were measured for each animal, it was necessary to combine two to five animals in a sample to measure body mass, C and N. A total of 332 CV and 278 CVI copepods (23–30 animals per tank) were measured for PL and OSV. A total of 345 CV and 334 CVI (27–29 animals per tank) were measured for DW, C, and N. We report results as the morphological and physiological state at newly molted stage CV. The remaining newly molted CV copepods were maintained in the treatment tanks until ~20% of the population became adult females. At that point, newly molted adult females were collected, photographed, and processed for further biometric measurements, or transferred to chambers for respiration rate measurements. By using the time of molt as a marker to identify age-within-stage, this novel method decreases variability by restricting measurements of body mass and vital rates to specific times during the copepod's development.

Oxygen consumption rates (OCR) of newly molted stage CV and adult females were made within 1 and 3 d, respectively, of molting. Copepods were collected from control and treatment tanks and sorted under a binocular microscope. Two to three copepods were transferred to experimental chambers (~4.8 mL) filled with seawater (containing no air spaces) from their respective tanks. Experimental chambers were sealed with a ground glass top in which there was a small hole (0.4 mm) to accommodate an oxygen-sensitive microelectrode. Dissolved oxygen concentrations were measured with a Clark-type oxygen microelectrode (Unisense). The electrode was calibrated with 0.2-μm filtered seawater bubbled for a minimum of 1 h to set the 100% dissolved oxygen calibration point. The anoxic calibration point (0% O_2) was determined by placing seawater into a silicone tube that was immersed in a solution of 0.1 M sodium ascorbate and 0.1 M sodium hydroxide for over 4 h. Oxygen measurements were made at the respective treatment temperature in a ThermoScientific water bath (Model A10B with thermostat SC100 ± 0.01°C). Oxygen concentrations within the chambers were measured every 2 s for up to 1.5 h. Oxygen concentration never decreased by more than 20% below saturation. Control chambers without animals were used to monitor oxygen changes due to microbial/algal respiration. Oxygen consumption was computed as the difference between the beginning and end of the incubation, corrected for changes in the control bottles. Data were normalized per unit DW obtained from direct measurements.

Stage CV and adult females from the control and treatment containers were sorted under a binocular microscope for analysis of fatty acids. The selected individuals were frozen in liquid nitrogen, stored at −80°C and then vacuum freeze-dried and shipped to the laboratory of M. Arts (Ryerson University, Canada) for analysis. Fatty acids were analyzed according to methods described in Hixson et al. (2016). Briefly, copepods were freeze-dried, weighed to the nearest microgram, and then total lipid was extracted using a slightly modified Folch et al. (1957) method, as described in McMeans et al. (2012). Each sample was extracted ×3, using 2 mL of 2:1 (vol/vol) chloroform : methanol and pooled, after which polar impurities were removed by adding 1.6 mL NaCl solution (0.9% wt/vol) (which was discarded following centrifugation). The resulting lipid-containing solvent was concentrated to 2 mL and 2 aliquots (100 μL each) were removed and evaporated to dryness to quantify total lipid gravimetrically. Fatty acids in the lipid extracts were derivatized to fatty acid methyl esters (FAME) using sulfuric acid as the catalyst (Christie 2003). The FAME were then extracted ×2 using hexanes: diethyl ether (1 : 1; vol/vol), after which they were dried under a gentle stream of extra dry nitrogen gas. The FAME were separated and analyzed using a gas chromatograph (GC) (Shimadzu-2010 Plus) equipped with an SP-2560 column (Sigma-Aldrich). All solvents used in the extraction and FAME derivatization procedures were of high-purity HPLC grade (>99%). The FAME were identified and quantified by retention time matching and a five-point calibration curve, respectively, using a reference standard (GLC-463, Nu-Chek Prep, Inc.). A known concentration of five alpha-cholestane (C8003, Sigma-Aldrich) was added to each sample prior to extraction to act as a surrogate internal standard to estimate extraction and instrument

recovery efficiency. Individual fatty acid contents were expressed as percent (molar) of total quantified (FAME). These data were arcsin square root transformed prior to statistical analysis.

Statistical analysis

Data were tested for normality (Shapiro–Wilk) and equal variance before testing for differences between the treatments (SigmaPlot V.11). If the data met the assumption of the ANOVA they were tested using a three-way full factorial ANOVA with replication (three tanks). Biological endpoints examined in the ANOVA included prosome length, OSV, DW, carbon (C) and nitrogen (N), mass. Patterns in biological variables and interactions with treatments were examined at the beginning of stages CV and recently molted CVI. Prosome length was included as a cofactor in the models to account for the size effect when evaluating DW, OSV, C, N. Separate models were calculated for each stage (early CV and late CV [recent molt to CVI]). OCR was normalized to C and was analyzed according to stage.

Fatty acid (FA) data were analyzed using discriminant analysis (DA). The aim was to investigate which individual FA contributed to the separation of pCO_2 treatment-temperature groups (four groups) rather than for predictive purposes. The number of variables (FA) in the analysis were reduced to be less than the sample size of the smallest group. To do this, we carried out an initial DA including all of the analyzed FA (21), then removed the ones that had lower contributions. We then picked the FA that were most ecologically relevant for the copepods. Assumptions of homogeneity of variance were satisfied (Bartlett test, $p > 0.05$). Data departed slightly from the assumption of multivariate normality which was evaluated graphically (QQ plot). An unsaturation index (UI) was calculated as the sum of the product of each fatty acid times its number of double bonds. All statistics and data analyses were calculated using the statistical software R (R Core Team 2019) and JMP (JMP, Version 16, SAS Institute Inc., 1989–2021). The significance level was $p \leq 0.05$.

Results

The experimental conditions were monitored daily during the 29 d (16°C) to 37 d (12°C) long experiment (Table 1). Food concentration in each tank was maintained above 600 μg C L^{-1}. Temperature and pCO_2 were maintained at nominal levels with low variability (Table 1). Mean pH was within 1% of cold ambient and warm treatment values.

Development rate of *C. finmarchicus* was significantly faster at 16 than at 12°C (ANCOVA: $p < 0.01$, Fig. 1) but there was no difference in developmental rates between pCO_2 concentrations within temperature treatments (Fig. 1). Development time to the midpoint of stage CIV (stage 9.5; Fig. 1) and Stage CV (stage 10.5; Fig. 1) was 24 and 29 d, respectively, at 12°C and 19 and 24 d, respectively, at 16°C.

All biological endpoints were significantly different between the beginning of stage CV and the beginning of CVI (Table 2, S1–S5). CVI copepods were significantly longer (PL), heavier (DW), contained more C and N, and had a larger oil sac volume (OSV). At 12°C and 600 μatm pCO2 copepods increased in PL from 2.0 mm at CV to 2.36 mm at CVI, an increase of 18%. During this single stage, copepods also increased 86% in DW, 71% in C, 47% in nitrogen, and 93% in OSV. At 16°C, copepods showed a similar increase in all of the biological endpoints. However, at the beginning of the CV stage, copepods were significantly smaller at 16°C and despite the rapid growth during the CV stage, they remained significantly smaller than the animals raised at 12°C. Because of the large increases in all of the biological endpoints, it was critical to design the experiment such that differences due to treatment effects were within a well-prescribed stage increment. In the following paragraphs, we compare the same biological endpoints within 12 h of reaching each stage so that the cumulative effects of temperature and pCO_2—independently and/or in combination—could be discriminated.

Prosome length (PL), at the beginning of the stage CV, and the beginning of CVI was significantly higher in copepods reared at 12 than at 16°C (Fig. 2; Table 2, S1; $p < 0.001$, for both stages). At the beginning of CV, copepods at 12°C were on average 7% longer than when reared at 16°C. At the beginning of CVI, copepods at 12°C were on average 6% longer than when reared at 16°C. Neither stage showed a significant direct pCO_2 effect on PL ($p = 0.28$) .

Temperature and pCO_2 had a significant direct and interactive effect on DW. Strong temperature effects produced heavier copepods at 12°C and at elevated pCO_2 at both copepod stages (Table 2, S2; $p < 0.001$, for both stages). At the beginning of CV and CVI, copepods reared at 12°C were on average 29% and 27% heavier, respectively than at 16°C. Elevated pCO_2 alone also produced larger copepods, independent of temperature. CV and CVI stage copepods were on average 11% and 10% larger, respectively, when reared at high pCO_2 compared to ambient $pCO2$. When combined, lower temperatures (12°C) and elevated pCO_2 resulted in copepods that were 44% and 38% heavier, respectively, than at high temp and ambient pCO_2 (Table 2). Plotting DW as a function of PL shows that the increased DW was independent of the increased PL (Fig. 3.). The copepods at low temperatures and high pCO_2 did not just get longer, they also became heavier (DW) at a given PL.

OSV showed a significant response to temperature and an interactive effect between temperature and pCO_2 (Table 2, S3). At 12°C, the OSVs were 67% and 43% larger than at 16°C for the CV and CVI, respectively. There was an interactive effect of elevated pCO_2 and temperature on OSV. At 12°C, copepods in the high pCO_2 treatment had significantly higher OSV (41% and 39% larger for CV and CVI, respectively) than at low pCO_2. When normalized to PL (OSV/PL; Fig. 4), the

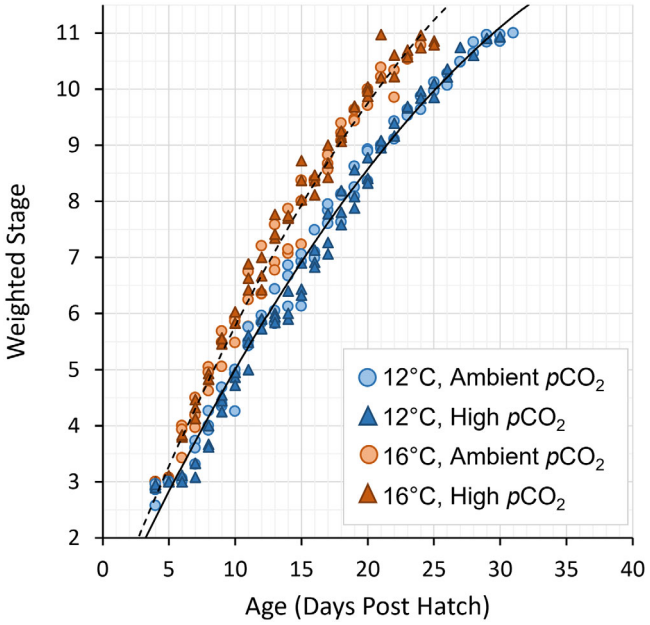

Fig. 1. Stage progression of *C. finmarchicus*. OA controls, and treatments shown by weighted stage value. The weighted stage value determined at each sampling date is equal to the sum of each stage fraction multiplied by its weight (N1 = 1, N2 = 2, N3 = 3…C1 = 7, C2 = 8, C3 = 9…C6 = 12). Red lines: warm (16°C); blue lines: lower (12°C) temperatures. Circles: ambient CO_2 (~600 μatm; pH 7.85); diamonds: high pCO_2 (~1100 μatm; pH 7.65) treatments. Values are fit with a polynomial with intercept at 0 and analyzed with ANCOVA on log-transformed data. The statistical analysis excludes slower development in early (<4) and late (>10) stages in order to achieve normal distribution of residuals. Water chemistry for all treatments is provided in Table 1.

OSV of the newly molted CV and CVI stages was significantly larger at the lower temperature. Thus, copepods at the same PL contained larger oil sacs when reared at lower temperatures. In contrast, there was no direct effect of pCO_2 on the OSV/PL ($p = 0.6$).

Carbon (C) showed a similar response to temperature and pCO_2 as DW. Total C content for both copepod stages was higher at 12 than at 16°C. The C content was 42% and 27% greater at 12 than at 16°C for the CV and CVI, respectively (Table 2). Elevated pCO_2, independent of temperature, increased the C content of the copepods by an additional 15% and 8%, respectively. When normalized to PL (Fig. 5), the C of the newly molted CV stage was significantly larger at the lower temperature and higher pCO_2. Thus, copepods at the same PL had larger C content when reared at lower temperatures and higher pCO_2.

In contrast to C, there was a significant effect of temperature on nitrogen content but no independent effect of pCO_2 (Supplementary Table S5). At 12°C, CV and CVI had 20% and 11% greater N than at 16°C.

There was a significant stage, temperature, and pCO_2 effect on mass-specific oxygen consumption rates (MS-OCR). MS-OCR (nmolO_2 h^{-1} $\mu g\ C^{-1}$) was higher in stage CVs than in the stage CVIs (newly molted CVI-adult females) (three-way ANOVA; $F_{1,23} = 58.5$; $p < 0.001$; Fig. 6). MS-OCR was significantly higher at 16 than at 12°C for both stages (three-way ANOVA; $F_{1,23} = 178.1$; $p < 0.001$—verified with a post hoc test; Supplementary Table S6). MS-OCR increased by 48–68% when temperature increased from 12°C to 16°C, for both stages. In contrast, increased pCO_2 significantly decreased MS-OCR (three-way ANOVA; $F_{1,23} = 10.3$; $p < 0.01$). Early stage CV showed a ~30% (12°C) and 25% (16°C) decrease in MS-OCR at the higher pCO_2. The MS-OCR for CVIs' decreased by 14% at 12°C and increased by ~5% at 16°C.

While we found no significant differences in mean FA concentrations between treatments (ANOVA, $p > 0.4$; Supplementary Table S7; Supplementary Fig. S1), some overall patterns appeared

Table 2. Effects of temperature (12°C and 16°C) and pCO_2 (~600 and 1100 μatm) on the means of body size measurements of stage CV *C. finmarchicus*, from entrance to exit molts. PL: prosome length (mm); DW: dry mass (μg); C: carbon mass (μg); N: nitrogen mass (μg); OSV: Oil sac volume (mm^3). Reported values are means (±SD) from three replicate tanks).

	At molt to CV		At molt to CVI	
12°C	Ambient	High	Ambient	High
PL (mm)	2.00 ± 0.04	2.06 ± 0.03	2.36 ± 0.03	2.41 ± 0.04
DW (μg)	94.2 ± 12.5	113.6 ± 17.0	175.4 ± 22.0	221.3 ± 33.1
C (μg)	44.5 ± 4.70	55.9 ± 9.81	76.3 ± 6.89	92.8 ± 9.27
N (μg)	9.36 ± 0.68	10.01 ± 0.58	13.73 ± 1.49	15.27 ± 0.98
OSV (mm^3)	0.029 ± 0.008	0.041 ± 0.008	0.056 ± 0.012	0.078 ± 0.020
16°C	Ambient	High	Ambient	High
PL (mm)	1.91 ± 0.05	1.90 ± 0.04	2.27 ± 0.06	2.25 ± 0.04
DW (μg)	79.0 ± 4.09	82.0 ± 9.05	160.3 ± 11.28	152.8 ± 9.78
C (μg)	34.1 ± 1.51	36.6 ± 3.70	68.2 ± 6.36	64.5 ± 7.88
N (μg)	7.55 ± 0.74	8.51 ± 1.70	13.42 ± 1.12	12.65 ± 0.56
OSV (mm^3)	0.021 ± 0.001	0.021 ± 0.006	0.048 ± 0.008	0.046 ± 0.009

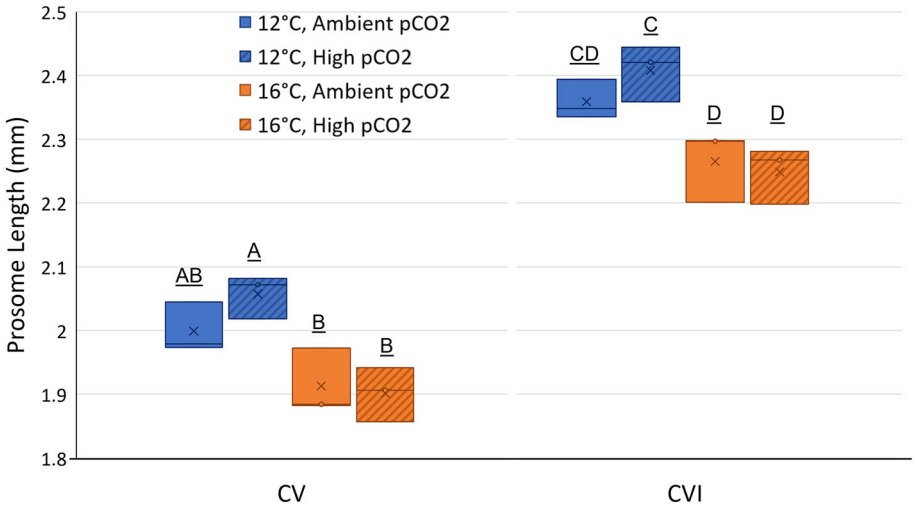

Fig. 2. Prosome length (PL) of *C. finmarchicus* reared at low and higher temperatures (12°C, 16°C) and pCO_2 levels of ambient (600 μatm) and high (1100 μatm) concentrations. Uppercase letters indicate pairwise differences; bars that have different letters are statistically different (Tukey's post hoc, $p \leq 0.05$, following ANOVA; Supplementary Table S1).

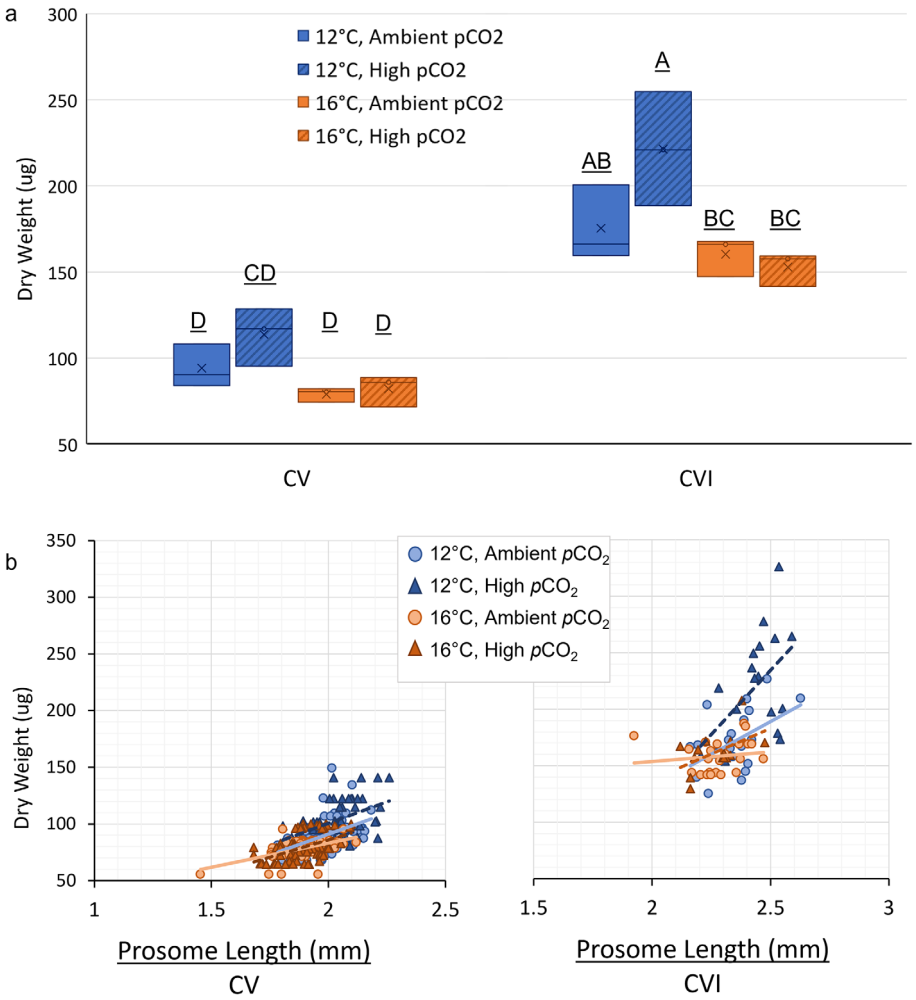

Fig. 3. (**a**) Dry weight (DW) of *C. finmarchicus* reared at lower and higher temperatures (12°C, 16°C) and pCO_2 levels of ambient (600 μatm) and high (1100 μatm) concentrations. Uppercase letters indicate pairwise differences; bars that have different letters are statistically different (Tukey's post hoc, $p \leq 0.05$, following ANOVA; Supplementary Table S2). (**b**) Dry weight (DW) as a function of prosome length (PL) for *C. finmarchicus* reared at lower and higher temperatures (12°C, 16°C) and pCO_2 levels of ambient (600 μatm) and high (1100 μatm) concentrations. Left panel is CV, right panel is CVI.

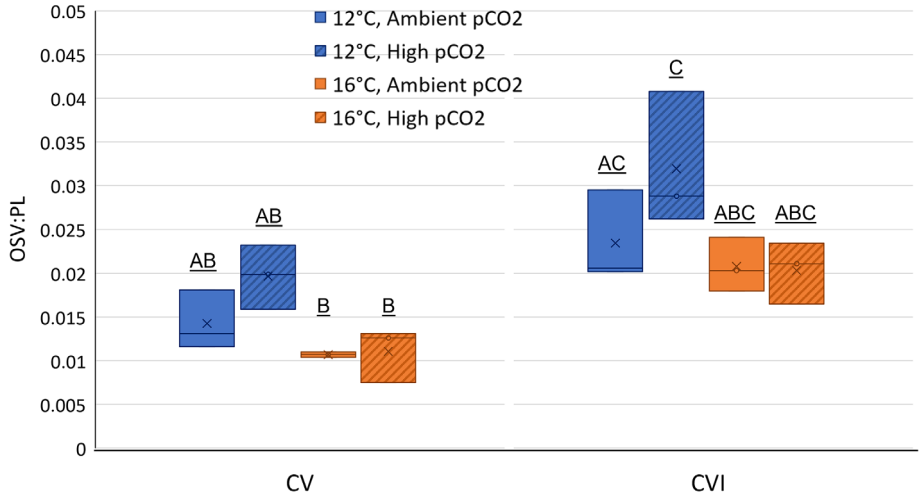

Fig. 4. Oil sac volume (OSV) normalized to prosome length (PL) of *C. finmarchicus* reared at lower and higher temperatures (12°C, 16°C) and pCO_2 levels of ambient (600 μatm) and high (1100 μatm) concentrations. Uppercase letters indicate pairwise differences; bars that have different letters are statistically different (Tukey's post hoc, $p \leq 0.05$, following ANOVA; Supplementary Table S3).

in a discriminant analysis (DA). In a DA of nine prominent FA (Fig. 7a), differences between ambient and pCO_2 treatments were discriminated mainly by the first discriminant function (LD1) and temperature differences were discriminated mainly by LD2. The two FA that contributed the most to pCO_2 treatment (LD1) were 16:0 and 18:3n−3 (ALA) while 16:0, 18:1n−9, and 18:2n−6 contributed the most to temperature differences (LD2). The CA (cold, ambient pCO_2) group was well separated from the three other groups (CH, WA, and WH) (Fig. 7b). Examination of LD2 indicates that the colder conditions were mainly associated with an increase in 16:0, 18:3n−6, and 18:1n−9. The higher temperature, and pCO_2 conditions were mainly characterized by increases in 18:2n−6 and a decrease in 18:1n−9 and 18:0. Differences in pCO_2 treatment were only evident at lower temperature—groups were clearly separated on the plot (Fig. 7b). While the warmer temperature groups overlapped. These differences in pCO_2 in the cold condition were mainly characterized by 16:0 and 18:3n−3: copepods raised at higher pCO_2 had a relatively higher 18:3n−3 and a lower 16:0, while the opposite was true for copepods raised at ambient pCO_2. There was a large overlap between both higher temperature treatments, whereas the low temperature-high pCO_2 treatment (CH) was characterized by relatively higher concentrations in 18:3n−6 and 18:1n−9 compared to the CA. The unsaturation index (UI) was not

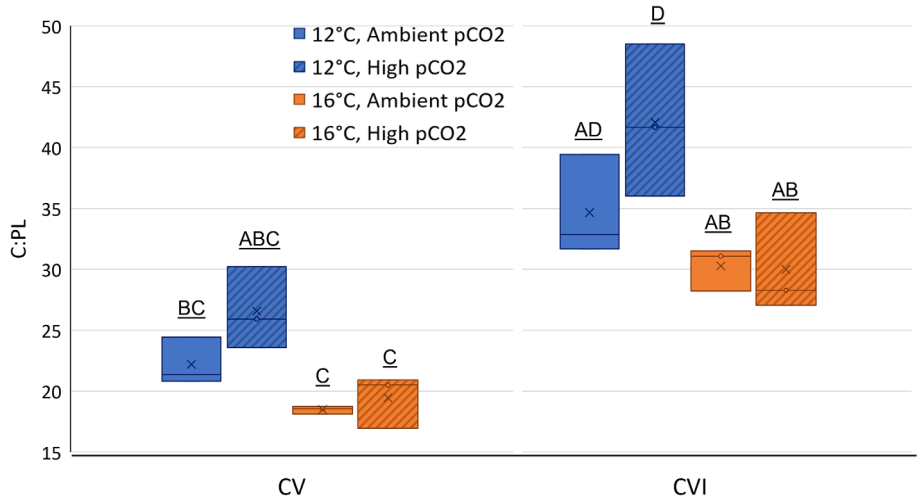

Fig. 5. Carbon (C) content normalized to prosome length (PL) of *C. finmarchicus* reared at lower and higher temperatures (12°C, 16°C) and pCO_2 levels of ambient (600 μatm) and high (1100 μatm) concentrations. Uppercase letters indicate pairwise differences; bars that have different letters are statistically different (Tukey's post hoc, $p \leq 0.05$, following ANOVA; Supplementary Table S4).

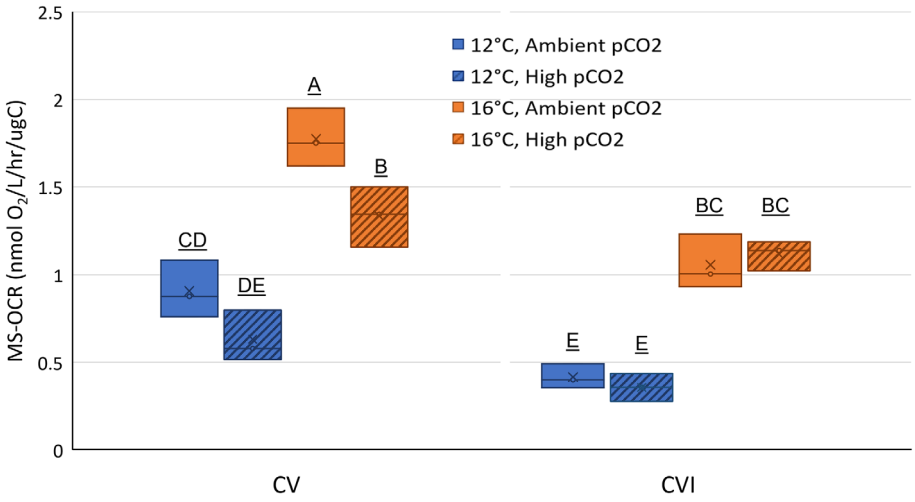

Fig. 6. Mass-specific oxygen respiration rate (MS-OCR) of CV and CVI *C. finmarchicus* reared at lower and higher temperatures (12°C, 16°C) and pCO_2 levels of ambient (600 μatm) and high (1100 μatm) concentrations. Uppercase letters indicate pairwise differences; bars that have different letters are statistically different (Tukey's post hoc, $p < 0.05$, following ANOVA; Supplementary Table S6).

significantly different among ambient and treatment conditions with respect to both temperature and pCO_2.

Discussion

C. finmarchicus increased in PL by 18% and its DW and OSV increased by ~100% from recently molted (<24 h) CV to recently molted (<24 h) CVI stage of development. Thus, small differences in the age of the copepods within a stage is a potential source of large variability in size-dependent vital rate measurements. Isolating newly molted CV and CVI stage copepods for measurements reduced the variability that arises from sampling rapidly growing individuals of unknown age within a developmental stage. By comparing biological endpoints, we were able to assess the impact of temperature and pCO_2 on the growth, metabolism, C and N mass, and lipid accumulation during this rapidly changing developmental stage. Our results confirm the preliminary finding reported in Runge et al. (2016) of a significantly larger body mass of *C. finmarchicus* reared at lower temperatures (12°C) and at higher pCO_2 concentration. As development times were indistinguishable between pCO_2 treatments, these results demonstrate that *C. finmarchicus* growth rates during CV were significantly higher under elevated pCO_2 (lower pH) conditions. Overall, lower temperatures and higher pCO_2 produced heavier (DW) adult females with a larger oil sac volume (OSV) and a concomitant increase in both C and N content. These results support the conclusion that the scope for growth for *C. finmarchicus* is more favorable at lower temperatures in the high pCO_2 treatment. *C. finmarchicus*, like other crustaceans, generally is more negatively affected by warming than by decreased pH (Runge et al. 2016; Waller et al. 2017; Pedersen and Hanssen 2018). However, this study also finds increased pCO_2 interacts with cooler temperature to produce heavier and more lipid rich adults.

This result represents one of the few reported positive effects of OA on physiological rate processes in a planktonic copepod. Engström-Östa et al. (2014) observed that egg production rates of *Acartia bifilosa* increased at low pH (7.6 decreasing to 7.2) relative to the ambient controls (7.9 decreasing to 7.5). However, the incubation exposures were short (38–42 h) and the effects of temperature and longer-term exposure were not investigated. McLaskey et al. (2019) observed that *Acartia hudsonica* nauplii developed faster at elevated pCO_2 (1200 μatm) at 12°C but not at 17°C, although this result could not be conclusively attributed to pCO_2 in isolation. In longer-term rearing experiments, Pedersen et al. (2014) suggested that the scope for growth of stage CV *C. finmarchicus* at a pCO_2 of 1100 μatm was approximately 22% higher (their fig. 2: mean of three tanks) than at ambient levels (420 μatm), although the result was not statistically significant.

There are at least three possible mechanistic explanations for the increased DW, C, and lipid content of copepods raised at higher pCO_2; (1) Increased ingestion and/or assimilation rates; (2) decreased energetic costs of maintaining the same metabolic rate; or (3) pCO_2-related increase in food quality that translated into higher growth. These mechanisms are not necessarily mutually exclusive.

While we did not measure ingestion rates in this study, previous work showed no effects of OA on ingestion rates of *C. finmarchicus* (Hildebrandt et al. 2016; Runge et al. 2016), *C. glacialis* (Hildebrandt et al. 2014), or in *A. hudsonica* (McLaskey et al. 2019).

Our data support the hypothesis that high pCO_2 lowers metabolic costs, resulting in increased growth and lipid

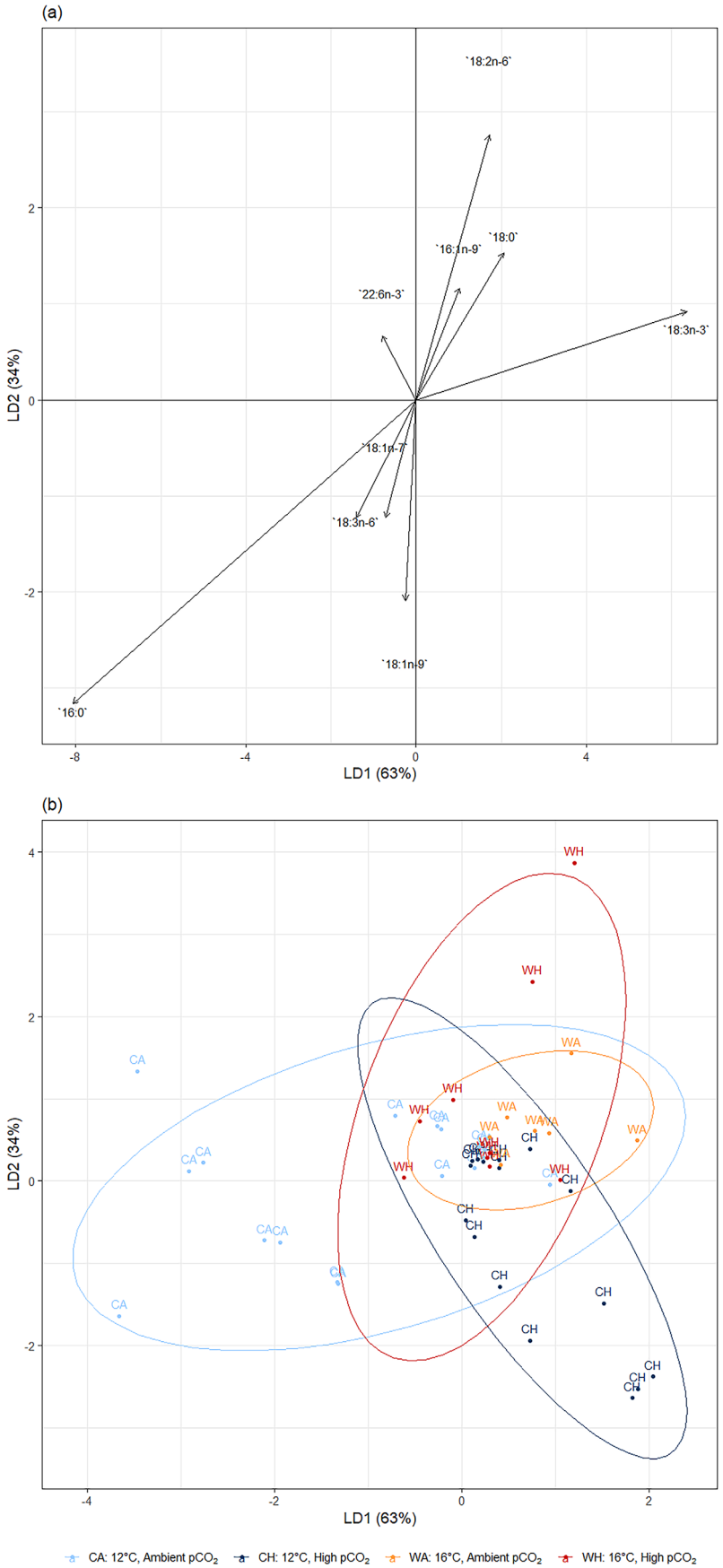

(Figure legend continues on next page.)

storage. Pörtner et al. (2004) suggested that decreased extracellular pH reduces ion channel pumping. Decreasing extracellular pH slows down the rate of H+ equivalent ion exchange by both Na^+/H^+- and Na^+- dependent Cl^-/HCO^{3-}-transporters which are responsible for the regulation of the intracellular acid–base status. Less sodium needs to be pumped by the Na^+/K^+-ATPase, thus diminishing the energy requirements of acid–base regulation. We observed lower MS-OCR at lower temperatures and higher pCO_2. The added benefit of elevated $pCO2$, however, was undetected (masked) at higher temperatures. At 16°C, the MS-OCR for the newly molted CVs was ~ 50% higher than at 12°C. Assuming a respiratory quotient of 0.82 (Ikeda 1985; Uye 1991; Schukat et al. 2013;), an average C content per copepod of 50.2 and 35.4 μg C at 12°C and 16°C, respectively, early CVs would respire ~ 18% of their body carbon per day (BC d^{-1}) at 12°C and 36% at 16°C. This implies that the lower metabolic costs at 12°C conserved resources that fueled more rapid growth and higher lipid storage. Elevated pCO_2 at 12°C further decreased the MS-OCR of the CVs. At 12°C and ambient pCO_2 levels, 21% of the BC d^{-1} was respired and at high pCO_2 only 15% of the BC d^{-1} was respired. A similar effect of pCO_2 was found at 16°C at which percentage BC d^{-1} consumed decreased from 43% to 30% from ambient to high pCO_2. This lower metabolic rate at 12°C, coupled with high pCO_2, led to significantly larger (PL), heavier (DW), and higher lipid reserves (OSV) by the time the animals molted to CVI (adult females). At the CVI stage, temperature showed a similar effect on metabolic rate. At 12°C, CVIs respired 10% BC d^{-1} while at 16°C that increased to 26% BC d^{-1}. At 12°C, elevated pCO_2 lowered MS-OCR, but at 16°C there was no added effect of increased pCO_2. The lower metabolic cost appears to occur within a relatively narrow range of higher pCO_2 and ambient temperatures (Pedersen and Hanssen 2018).

Whiteley (2011) concludes that there is considerable variability in the response of crustaceans to pCO_2, but suggests that species exposed to a broad range of environmental conditions should be better equipped physiologically to tolerate increased pCO_2 and lower pH. In those organisms that are tolerant to pCO_2 oscillations, increased pCO_2 caused a decrease in metabolic rate (Pörtner et al. 2004). In general, pCO_2 concentrations increase with depth in the water column in all the oceans due to the biological pump (Goyet et al. 2000—plotted by Hofmann et al. 2013). As vertical migrators, older life stages of *C. finmarchicus* experience daily change between the ambient pCO_2 levels at the surface and higher pCO_2 levels at depth (up to 250 m: Plourde et al. 2001) and, in addition, stage CV *C. finmarchicus* overwinter for months in deep water. In the N. Atlantic at the depths at which diapause occurs (500–2000 m: Heath et al. 2008), pCO_2 can reach 800–1000 μatm (Murray 2004).

Although the high turnover rates in the culture tanks minimized exposure of the algal food source to the different $pCO2$ treatment levels, it is possible that rapid changes in food quality may have occurred. In laboratory experiments, OA driven declines in both total FA and the ratio of long-chain polyunsaturated to saturated FA in the diatom *Thalassiosira pseudonana*, grown at high pCO_2 levels, constrained growth and reproduction of the copepod *Acartia tonsa* that were fed on them (Rossoll et al. 2012). Furthermore, lower quality food, due to OA, also decreased trophic transfer efficiency from phytoplankton to zooplankton by ~ 50% and caused a commensurate decrease in zooplankton reproduction rates (Cripps et al. 2014, 2016). Since 10–20% of essential biomolecules in primary producers are incorporated into new biomass at the next trophic level, a decline of food quality in primary producers will impact the zooplankton that prey on them. Alternately, in some cases, high pCO_2 levels may lead to increased algal growth rates which, in turn, may decrease the negative effects of OA on invertebrates that feed on phytoplankton (Li and Gao 2012; Thomsen et al. 2013; Garzke et al. 2016). In addition, although both temperature and pCO_2 can affect the quality and quantity of marine algae (Reum et al. 2015), accompanying changes in seston community composition, driven by phosphate and silicate limitation, may also be affected by pCO_2 levels (Bermúdez et al. 2016). Such changes in community composition of seston can influence both total lipid levels as well as the underlying abundance of individual fatty acids and lipid classes (Bermúdez et al. 2016). This is because seston community composition is a key driver of overall abundance and distribution of individual fatty acids in seston (Galloway and Winder 2015). We conclude that, although differences in the metabolic rate (MS-OCR) of *C. finmarchicus*, due to temperature and pCO_2 are sufficient to explain the observed changes in copepod size, lipid content, and growth rate that we observed in the lab, the indirect effects of climate change (i.e., both temperature and pCO_2 drivers) on food quality may mask these results in the field.

C. finmarchicus is a key component of North Atlantic food webs. Over the last five decades, the species distributional range in the northeast Atlantic has contracted while the range of its southern sibling species, *C. helgolandicus*, has expanded

(Figure legend continued from previous page.)

Fig. 7. (**a**) Standardized discriminant coefficients, showing weight attributed to each of nine prominent fatty acids and extent of differentiation among temperature-pCO_2 treatment conditions: cold-ambient (CA; 12°C, 600 μatm), cold-high (CH; 12°C, 1100 μatm, warm-ambient (WA; 16°C, 600 μatm, warm-high (WH; 16°C, 1100 μatm,) in *C. finmarchicus*. The greater the coefficient, the larger the contribution of its associated variable to group differentiation. (**b**) Observations plotted using the two discriminant functions (% variance explained). Ellipses are the 95% confidence interval of the group means.

correspondingly (Beaugrand et al. 2002; Strand et al. 2020). This shift has been linked to rising ocean temperatures (Hinder et al. 2014). A further biogeographic shift is expected as temperature continues to increase (Maar et al. 2013). As ocean temperatures continue to increase, the decrease in the size of *C. finmarchicus*, its lipid content, and the concentration of essential FA in combination with decreasing abundance (Grieve et al. 2017) will have consequential effects on higher trophic levels that depend on this copepod as a food source. In the future ocean, copepods and other planktonic taxa will need to respond to change, not only in temperature but also to pCO_2 and corresponding pH, change in food availability and quality, as well as other stressors (Breitburg et al. 2015; McLaskey et al. 2019; Meyers et al. 2019). Pan et al. (2015) emphasized a need for research on biochemical mechanisms of response at the cellular level and the limits of their adaptive capacity as an approach to gaining insight into how the future ocean environment will affect marine species. The results reported here are an example of the level of knowledge and understanding needed to make accurate predictions of future biological effects of climate change on planktonic copepods.

Data availability statement

Data are available from ResearchGate: 10.13140/RG.2.2.36766.82242

References

Andersen, S., E. S. Grefsrud, and T. Harboet. 2013. Effect of increased pCO_2 level on early shell development in great scallop (*Pecten maximus* Lamarck) larvae. Biogeosciences **10**: 6161–6184. doi:10.5194/bg-10-6161-2013

Anger, K. 2001, p. 1–405. *In* R. Vonk [ed.], The biology of decapod crustacean larvae, Crustacean issues, v. **14**. A. A. Balkema.

Bailey, A., and others. 2016. Early life stages of the Arctic copepod *Calanus glacialis* are unaffected by increased seawater pCO_2. ICES J. Mar. Sci. **74**: 996–1004.doi:10.1093/icesjms/fsw066

Bailey, A., and others. 2017. Regulation of gene expression underlies tolerance of the Arctic copepod *Calanus glacialis* to CO_2-acidified seawater. Ecol. Evol. **7**: 7145–7160. doi:10.1002/ece3.3063

Beaugrand, G., P. C. Reid, F. Ibanez, J. A. Lindley, and M. Edwards. 2002. Reorganization of North Atlantic marine copepod biodiversity and climate. Science **296**: 1692–1694. doi:10.1126/science.1071329

Bermúdez, J. R., M. Winder, A. Stuhr, A.-K. Almén, J. Engström-Öst, and U. Riebesell. 2016. Effect of ocean acidification on the structure and fatty acid composition of a natural plankton community in the Baltic Sea. Biogeosciences **13**: 6625–6635. doi:10.5194/bg-13-6625-2016

Breitburg, D. L., and others. 2015. And on top of all that… coping with ocean acidification in the midst of many stressors. Oceanography **28**: 48–61. doi:10.5670/oceanog.2015.31

Browman, H. I. 2017. Towards a broader perspective on ocean acidification research. ICES J. Mar. Sci. **74**: 889–894. doi:10.1093/icesjms/fsx073

Buren, A. D., M. Koen-Alonso, P. Pepin, F. Mowbray, B. Nakashima, G. Stenson, N. Ollerhead, and W. A. Montevecchi. 2014. Bottom-up regulation of capelin, a keystone forage species. PLoS One **9**: e87589. doi:10.1371/journal.pone.0087589

Caldeira, K., and M. E. Wickett. 2003. Anthropogenic carbon and ocean pH. Nature **425**: 365.

Christie, W. W. 2003. Preparation of derivates of fatty acids, p. 205–225. *In* W. W. Christie [ed.], Lipid analysis: Isolation, separation and structural analysis of lipids, 3rd ed. J. Barnes and Associates.

Cripps, G., P. K. Lindeque, and K. J. Flynn. 2014. Have we been underestimating the effects of ocean acidification in zooplankton? Glob. Change Bio. **20**: 3377–3385. doi:10.1111/gcb.12582

Cripps, G., K. J. Flynn, and P. K. Lindeque. 2016. Ocean acidification affects the Phyto-zoo plankton trophic transfer efficiency. PLoS ONE **11**: e0151739. doi:10.1371/journal.pone.0151739

Dickson, A. G. 2007. SOP7 determination of the pH of sea water using the indicator dye m-cresol purple, p. 191. *In* Guide to best practice for ocean CO2 measurements. PICES Special Publication.

Dickson, A. G., and F. J. Millero. 1987. A comparison of the equilibrium constants for the dissociation of carbonic-acid in seawater media. Deep-Sea Res. Part A-Oceanogr. Res. Pap. **34**: 1733–1743.

Engström-Östa, J., T. Holmbornc, A. Brutemarkab, H. Hogforsc, A. Vehmaab, and E. Gorokhovad. 2014. The effects of short-term pH decrease on the reproductive output of the copepod *Acartia bifilosa*—a laboratory study. Mar. Freshw. Behav. Physiol. **47**: 173–183. doi:10.1080/10236244.2014.919096

Fabry, V. J., B. A. Seibel, R. A. Feely, and J. C. Orr. 2008. Impacts of ocean acidification on marine fauna and ecosystem processes. ICES J. Mar. Sci. **65**: 414–432. doi:10.1093/icesjms/fsn048

Folch, J., M. Lees, and G. H. Sloane-Stanley. 1957. A simple method for the isolation and purification of total lipids from animal tissues. J. Biol. Chem. **226**: 497–509.

Frost, B. W. 1974. *Calanus marshallae*, a new species of calanoid copepod closely allied to the sibling species *C. finmarchicus* and *C. glacialis*. Mar. Biol. **26**: 77–99.

Galloway, A. W. E., and M. Winder. 2015. Partitioning the relative importance of phylogeny and environmental conditions on phytoplankton fatty acids. PLOS ONE **10**: e0130053. doi:10.1371/journal.pone.0130053

Garzke, J., T. Hansen, S. M. H. Ismar, and U. Sommer. 2016. Combined effects of ocean warming and acidification on

copepod abundance, body size and fatty acid content. PLoS One **11**: 22. doi:10.1371/journal.pone.0155952

Gledhill, D. K., M. M. White, J. E. Salisbury, H. Thomas, I. Mlsna, M. Liebman, B. Mook, and others. 2015. Ocean and coastal acidification off New England and nova scotia. Oceanography **28**: 182–197. doi:10.5670/oceanog.2015.41

Goyet, C., Healy, R. J., and J. P. Ryan. 2000. Global distribution of total inorganic carbon and total alkalinity below the deepest winter mixed layer depths, ORNL/CDIAC-127, NDP-076. Carbon Dioxide Information Analysis Center, Oak Ridge National Laboratory, US Department of Energy, Oak Ridge, TN.

Grieve, B. D., J. A. Hare, and V. S. Saba. 2017. Projecting the effects of climate change on *Calanus finmarchicus* distribution within the U.S. Northeast Continental Shelf. Sci. Rep. **7**: 6264. doi:10.1038/s41598-017-06524-1

Heath, M. R., and S. H. Jónasdóttir. 1999. Distribution and abundance of overwintering *Calanus finmarchicus* in the Faroe–Shetland Channel. Fish. Oceanogr. **8**: 40–60.

Heath, M. R., and R. G. Lough. 2007. A synthesis of large-scale patterns in the planktonic prey of larval and juvenile cod (*Gadus morhua*). Fish. Oceanogr. **16**: 169–185. doi:10.1111/j.1365-2419.2006.00423.x

Heath, M. R., and others. 2008. Spatial demography of *Calanus finmarchicus* in the Irminger Sea. Prog. Oceanogr. **7**: 39–88. doi:10.111/j.1365-2419,2006.00723.x

Hildebrandt, N., B. Niehoff, and F. J. Sartoris. 2014. Long-term effects of elevated CO2 and temperature on the Arctic calanoid copepods *Calanus glacialis* and *C. hyperboreus*. Mar. Pollut. Bull. **80**: 59–70.doi:10.1016/j.marpolbul.2014.01.050

Hildebrandt, N., F. J. Sartoris, K. G. Schulz, U. Riebesell, and B. Niehoff. 2016. Ocean acidification does not alter grazing in the calanoid copepods *Calanus finmarchicus* and *Calanus glacialis*. ICES J. Mar. Sci. **73**: 927–936.doi:10.1093/icesjms/fsv226

Hinder, S. L., M. B. Gravenor, M. Edwards, C. Ostle, O. G. Bodger, P. L. M. Lee, and G. C. Hays. 2014. Multi-decadal range changes vs. thermal adaptation for north East Atlantic oceanic copepods in the face of climate change. Glob. Change Biol. **20**: 140–146. doi:10.1111/gcb.2013.20.issue-1

Hirche, H.-J. 1996. Diapause in the marine copepod, *Calanus finmarchicus*– A review. Ophelia **44**: 129–143.

Hixson, S. M., K. Shukla, L. G. Campbell, R. H. Hallett, S. S. Smith, L. Packer, and M. T. Arts. 2016. Long-chain omega-3 polyunsaturated fatty acids have developmental effects on the crop pest, the cabbage white butterfly (*Pieris rapae*). PLoS ONE. **11**: e0152264. doi:10.1371/journal.pone.0152264

Hofmann, A. F., E. T. Peltzer, and P. G. Brewer. 2013. Kinetic bottlenecks to chemical exchange rates for deep-sea animals—part 2: Carbon dioxide. Biogeosciences **10**: 2409–2425. doi:10.5194/bg-10-2409-2013

Ikeda, T. 1985. Metabolic rates of epipelagic marine zooplankton as a function of body mass and temperature. Mar. Biol. **85**: 1–11.

Jónasdóttir, S. H. 1999. Lipid content of *Calanus finmarchicus* during overwintering in the Faroe–Shetland Channel. Fish. Oceanogr. **8**: 61–72.

Lewis, E., D. Wallace, and L. J. Allison. 1998. CO2SYS - program developed for CO_2 system calculations. Carbon Dioxide Information Analysis Center.

Li, W., and K. Gao. 2012. A marine secondary producer respires and feeds more in a high CO_2 ocean. Mar. Poll. Bull. **64**: 699–703. DOI:10.1016/j.marpolbul.2012.01.033

Lindegren, M., M. Van Deurs, B. R. MacKenzie, L. Worsoe Clausen, A. Christensen, and A. Rindorf. 2018. Productivity and recovery of forage fish under climate change and fishing: North Sea sandeel as a case study. Fish. Oceanogr. **27**: 212–221.doi:10.1111/fog.12246

Maar, M., E. F. Moller, Z. Gurkan, S. H. Jonasdottir, and T. G. Nielsen. 2013. Sensitivity of *Calanus* spp. copepods to environmental changes in the North Sea using life-stage structured models. Prog. Oceanogr. **111**: 24–37. doi:10.1016/j.pocean.2012.10.004

McLaskey, A. K., J. E. Keister, K. L. Schoo, M. B. Olson, and B. A. Love. 2019. Direct and indirect effects of elevated CO2 are revealed through shifts in phytoplankton, copepod development, and fatty acid accumulation. PloS one **14**: e0213931.doi:10.1371/journal.pone.0213931

McMeans, B. C., M. T. Arts, and A. T. Fisk. 2012. Similarity between predator and prey fatty acid profiles is tissue dependent in Greenland sharks (*Somniosus microcephalus*): Implications for diet reconstruction. J. Exp. Mar. Biol. Ecol. **429**: 55–63.doi:10.1016/j.jembe.2012.06.017

Mehrbach, C., C. H. Culberson, J. E. Hawley, and R. M. Pytkowic. 1973. Measurement of apparent dissocation constants of carbonic acid in seawater at atmospheric pressure. Limnol. Oceanogr. **18**: 897–907.

Melle, W., J. Runge, E. Head, S. Plourde, C. Castellani, P. Licandro, J. Pierson, and others. 2014. The North Atlantic Ocean as habitat for *Calanus finmarchicus*: Environmental factors and life history traits. Progr. Oceanogr. **129**: 244–284. doi:10.1016/j.pocean.2014.04.026

Meyers, M. T., W. P. Cochlan, E. J. Carpenter, and W. J. Kimmerer. 2019. Effect of ocean acidification on the nutritional quality of marine phytoplankton for copepod reproduction. PLoS ONE **14**: e0217047. doi:10.1371/journal.pone.0217047

Murray, J. W. 2004. Ocean carbonate chemistry: The aquatic chemistry fundamentals, p. 1–24. *In* M. Follows and T. Oguz [eds.], The ocean carbon cycle and climate. Springer. doi:10.1007/978-1-4020-2087-2

Pan, T.-C. F., S. L. Applebaum, and D. T. Manahan. 2015. Energy allocation under ocean acidification. PNAS **112**: 4696–4701. doi:10.1073/pnas.1416967112

Pedersen, S. A., O. J. Hakedal, I. Salaberria, A. Tagliati, L. M. Gustavson, B. M. Jenssen, A. J. Olsen, and D. Altin. 2014. Multigenerational exposure to ocean acidification during food limitation reveals consequences for copepod scope for

growth and vital rates. Environ. Sci. Technol. **48**: 12275–12284.doi:10.1021/es501581j

Pedersen, S. A., and A. E. Hanssen. 2018. Ocean acidification ameliorates harmful effects of warming in primary consumer. Ecol. Evol. **8**: 396–404. doi:10.1002/ece3.3526

Pershing, A. J., and K. Stamieszkin. 2020. The North Atlantic ecosystem, from plankton to whales. Ann. Rev. Mar. Sci. **12**: 339–359.doi:10.1146/annurev-marine-010419-010752

Plourde, S., P. Joly, J. A. Runge, B. Zakardjian, and J. Dodson. 2001. Life cycle of *Calanus finmarchicus* in the lower St. Lawrence estuary: The imprint of circulation and late timing of the spring phytoplankton bloom. Can. J. Fish. Aquat. Sci. **58**: 647–658.

Pörtner, H. O., M. Langenbuch, and A. Reipschläger. 2004. Biological impact of elevated ocean CO_2 concentrations: Lessons from animal physiology and earth history. J. Oceanogr. **60**: 705–718. doi:10.1007/s10872-004-5763-0

Preziosi, B. M., J. A. Runge, J. P. Christensen, and R. J. Jones. 2017. The effect of pH and temperatures on hatching success of the marine planktonic copepod, *Calanus finmarchicus*. Mar. Biol. **164**: 218. doi:10.1007/s00227-017-3243-5

Quinn, B. K. 2017. Threshold temperatures for performance and survival of American lobster larvae: A review of current knowledge and implications to modeling impacts of climate change. Fish. Res. **186**: 383–396.doi:10.1016/j.fishres.2016.09.022

R Core Team (2019). R: A language and environment for statistical computing. R Foundation for Statistical Computing, Vienna, Austria. https://www.R-project.org/.

Record, N. R., and others. 2019. Rapid climate-driven circulation changes threaten conservation of endangered North Atlantic right whales. Oceanography **32**: 162–169.doi:10.5670/oceanog.2019.201

Reum, J. C. P., B. E. Ferris, P. S. McDonald, D. M. Farrell, C. J. Harvey, T. Klinger, and P. Levin. 2015. Evaluating community impacts of ocean acidification using qualitative network models. Mar. Ecol. Progr. Ser. **536**: 11–24. doi:10.3354/meps11417

Ross, R. M., and L. B. Quetin. 1988. Euphausia superba: A critical review of annual production. Comp. Biochem. Physiol. **90**: 499–505.

Rossoll, D., R. Bermudez, H. Hauss, K. G. Schulz, U. Sommer, and M. Winder. 2012. Ocean acidification-induced food quality deterioration constrains trophic transfer. Plos One **7**: e34737.doi:10.1371/journal.pone.0034737

Runge, J. A., D. M. Fields, C. R. S. Thompson, S. D. Shema, R. M. Bjelland, C. M. F. Durif, A. B. Skiftesvik, and H. I. Browman. 2016. End of the century CO2 concentrations do not have a negative effect on vital rates of *Calanus finmarchicus*, an ecologically critical planktonic species in North Atlantic ecosystems. ICES J. Mar. Sci. **73**: 937–950. doi:10.1093/icesjms/fsv258

Sargent, J. R., and R. J. Henderson. 1986. Lipids, p. 58–108. *In* E. D. S. Corner and S. C. M. O'Hara [eds.], The biological chemistry of marine copepods. Clarendon Press.

Schukat, A., L. Teuber, W. Hagen, N. Wasmund, and H. Auel. 2013. Energetics and carbon budgets of dominant calanoid copepods in the northern Benguela upwelling system. J. Exp. Mar. Biol. Ecol. **442**: 1–9.doi:10.1016/j.jembe.2013.01.024

Staudinger, M. D., and others. 2020. The role of sand lances (*Ammodytes* sp.) in the Northwest Atlantic Ecosystem: A synthesis of current knowledge with implications for conservation and management. Fish Fish. **21**: 522–556. doi:10.1111/faf.12445

Strand, E., E. Bagøien, M. Edwards, C. Broms, and T. Klevjer. 2020. Spatial distributions and seasonality of four Calanus species in the Northeast Atlantic. Prog. Oceanogr. **185**: 102344. doi:10.1016/j.pocean.2020.102344

Thomsen, J., I. Casties, C. Pansch, A. Körtzinger, and F. Melzner. 2013. Food availability outweighs ocean acidification effects in juvenile *Mytilus edulis*: Laboratory and field experiments. Glob. Change Biol. **19**: 1017–1027.doi:10.1016/j.jembe.2013.01.024

Uye, S. 1991. Temperature-dependent development and growth of the planktonic copepod *Paracalanus* sp. in the laboratory. Bull. Plankton Soc. Jpn, Spec. Vol: **627–636**.

Waller, J. D., R. A. Wahle, H. McVeigh, and D. M. Fields. 2017. Linking rising pCO_2 and temperature to the larval development and physiology of the American lobster (*Homarus americanus*). ICES J. Mar. Sci. **74**: 1210–1219. doi:10.1093/icesjmsfsw154

Wang, M., C. B. Jeong, Y. H. Lee, and J. S. Lee. 2018. Effects of ocean acidification on copepods. Aquat. Toxicol. **196**: 17–24.doi:10.1016/j.aquatox.2018.01.004

Whiteley, N. M. 2011. Physiological and ecological responses of crustaceans to ocean acidification. Mar. Ecol. Prog. Ser. **430**: 257–271.doi:10.3354/meps09185

Acknowledgments

David M. Fields received support from NSF award OCE-1220068 and NOAA-OAR-CPO-2011-2002561. Jeffrey A. Runge and Cameron R. S. Thompson were additionally supported by the National Science Foundation award OCE-1459087. Michael T. Arts received support from the Natural Sciences and Engineering Research Council (award #04537-2014). Additional funding for this work was provided by the Institute of Marine Research and the Fram Centre, Norway under Project #14591-02 to Howard I. Browman.

Submitted 17 December 2021
Revised 04 June 2022
Accepted 24 October 2022

Guest editor: Maarten Boersma